Draft version June 4, 2023
Typeset using LaTeX **twocolumn** style in AASTeX631

Photometric Analysis and Color-Magnitude Diagram of the Globular Cluster M3r

Sherry Yang,[1] Yasin A Chowdhury,[1] Andrew Carr,[1] and Jake Root[1]

[1] *Astronomy Department of University of Washington*

ABSTRACT

Among the numerous globular clusters that populate our Milky Way galaxy, the M3 globular cluster (also known as Messier 3 or NGC 5272) holds particular significance and has been a subject of intense study in the field of astronomy. In this paper, we present a detailed analysis of the globular cluster M3 using observations obtained in the B and V bands and the corresponding color index B-V. Our study aims to construct a Color-Magnitude Diagram (CMD) for M3, identifying its stellar populations and comparing our findings with previous studies. To achieve this, we employed the DAOPhot algorithm to perform star detection on the B and V band images.Subsequently, we conducted a cross-match between the two bands to establish correspondences and ensure reliable data. Using the resulting stellar catalogs, we constructed a CMD, plotting the magnitude of stars in the V band against their color index B-V. The CMD involved high luminosity features like red giant branch, asymptotic giant branch and horizontal branch. To validate our findings, we compared our CMD with previous studies on M3. However, we noticed a few discrepancies that could be attributed to variations in the observational data, photometric calibration, or stellar evolution models. These inconsistencies suggest potential avenues for improvement in future investigations.

Keywords: Photometric Analysis and Color-Magnitude Diagram of the Globular Cluster M3

1. INTRODUCTION

1.1. *Adequate background*

M3 is located in the constellation Canes Venatici and is estimated to be approximately 33,900 light-years (Goldsbury et al. 2010) away from Earth. It was first discovered by Charles Messier in 1764 and has since captivated astronomers with its striking appearance and rich stellar content.

One of the key reasons M3 has garnered significant attention is its age. Extensive studies have estimated the age of M3 to be around 11.4 billion years, making it one of the oldest known globular clusters in our Milky Way galaxy. Its ancient nature provides a crucial window into the early stages of stellar evolution and the formation of galaxies.

M3's stellar population comprises hundreds of thousands to millions of stars, densely packed within a relatively small region. The cluster exhibits a diverse range of stellar types, including main-sequence stars, red giants, blue stragglers, and white dwarfs. These stars represent different stages of stellar evolution, allowing astronomers to probe various astrophysical phenomena. Among these stages, the HB represents a critical evolutionary phase for low-mass stars in globular clusters. Understanding the properties and characteristics of HB stars provides valuable insights into stellar evolution, By studying the HB in M3, we gain a better understanding of the physical processes that govern stellar evolution in dense stellar environments.

Corresponding author: Sherry Yang
yyang35@uw.edu

1.2. *Purpose of study.*

M3 (NGC 5272) has been studied extensively photometrically. In optical colour-magnitude diagrams (CMDs), HB stars of M3 show a horizontal sequence, covering red HB, RR Lyrae (RRL), and blue HB ((Paez et al. 1990)), whereas HB stars of M13 show a vertical sequence, covering extreme HB, blue HB, and a very small number of RRL variables (Buonanno et al. 1994). The morphology of HB stars in M3 and M13 has served as the best suitable example of the long-standing "second parameter problem" for decades.(Egret et al. 1992)(199 1992)

Also, several research groups have conducted multi-band color-magnitude analyses on the M3 globular cluster, employing different observational datasets and analysis techniques to investigate various aspects of its stellar population. Kumar's group (Kumar et al. 2023). using observation data based on Globular Cluster UVIT Legacy Survey (GlobULeS) analyze Evolutionary status of hot stars in M3, and Hamrick's group (Hamrick et al. 2021) doing Characterization of NGC 5272 and other Globular Cluster based on multi-color bands based on Point Spread Function (PSF) photometry. Massari group (Massari et al. 2016) reports a double red giant branch on M3 based on photometry and CMD analyses .

Based on the previous works, we aim to reproduce the color-magnitude relationship, particularly focusing on the high luminosity range, as observed in previous studies of the M3 globular cluster. By replicating these color-magnitude relationships, we strive to validate and expand upon the findings from earlier research.

The study of Color-Magnitude Diagrams (CMDs) plays a crucial role in understanding the properties and evolution of stellar populations within a given astronomical system. CMDs provide a wealth of information, allowing astronomers to investigate various aspects of stellar astrophysics, galactic structure, and cosmology.Color-Magnitude Diagrams (CMDs) are fundamental tools in astrophysics, providing a visual representation of stellar populations within astronomical systems. This section highlights the significance of CMDs in scientific research, serving as a guide for understanding the subsequent discussions.

This paper includes the section of observations, containing the Photometric observations, Telescope and CCD camera details, and observation bands. The reduction procedures includes the reduction of bias and flat, and also a part about adjust the data based on VizieR catalog. Final part of this article is about the analysis of our HR diagram, and talks about the characteristics of the horizontal branch of M3.

2. OBSERVATIONS

2.1. *Location and equipment*

The observation made in The Apache Point Observatory. It is an astronomical observatory located in the Sacramento Mountains in Sunspot, New Mexico, United States, approximately 18 miles south of Cloudcroft (32°46'49"N 105°49'13"W). The observatory is operated by New Mexico State University (NMSU) and owned by the Astrophysical Research Consortium (ARC). Observation is taken by 0.5 m telescope: ARCSAT The ARC Small Aperture Telescope (ARCSAT) was previously called the Photometric Telescope (PT) when it was part of the SDSS project. It is a 0.5 m (20 in) reflecting telescope on an equatorial mount, with a single CCD camera cooled by a CryoTiger unit.

2.2. *Exposure times and spectral range*

Observations takes on the night 22th April. 10 min exposures on each bans (B,V,and SDSS r band) on our target: NGC5257 (RA: 13h 42m 11.62s Dec +28° 22' 38.2") (Harris 2010). The observation is taken on mid-night at the time target passing the Zenith, resulting the air-mass almost reaching one. This choice ensured optimal conditions for observing the M3 cluster, minimizing atmospheric interference and maximizing the clarity of the collected data. However, it is important to note that the observing night was cloudy, and the presence of clouds unavoidably affected the quality of the observations. Despite the presence of clouds, the temperature of the charge-coupled device (CCD) on the observer day was approximately -25C. This temperature range is considered suitable for producing reasonable observations.

Table 1: Information of Exposure

Filter	Exp_time	Airmass	Windows	Radius
bessel-B	600	1.0350	31.5'×31.5'	0.5m
bessel-V	600	1.0717	31.5'×31.5'	0.5m

On 22th April, the moon has a phase of 2.68 rad, and with a illumination of 0.05, and moon is not shown up on observable sky during the night. The effect of moon can be ignore.

In order to minimize the effect of equipment, corresponding to the observations, our group also took 8 flats on each bands, and 11 bias as total. These correction frames will be used to reduced the final observations.

3. REDUCTION AND CALIBRATION

3.1. *Reductions on Data*

The data reduction part includes two produces bias correction and flat correction. The effect of dark correction is negligible since the observing exposure time only 10 min, and it is small enough to ignore effect of dark correction. For bias correction. We collects 11 bias frames, and they capture the electronic offset and bias level of the detector. Bias frames should have a sufficient number of exposures to average out any random noise. It is advisable to take several bias frames to account for any variation in the bias level across the detector.To correct

Figure 1: Referenced Star Locations[1], Calibration on Magnitude[2], and Location Match Cross B,V Bands[3]

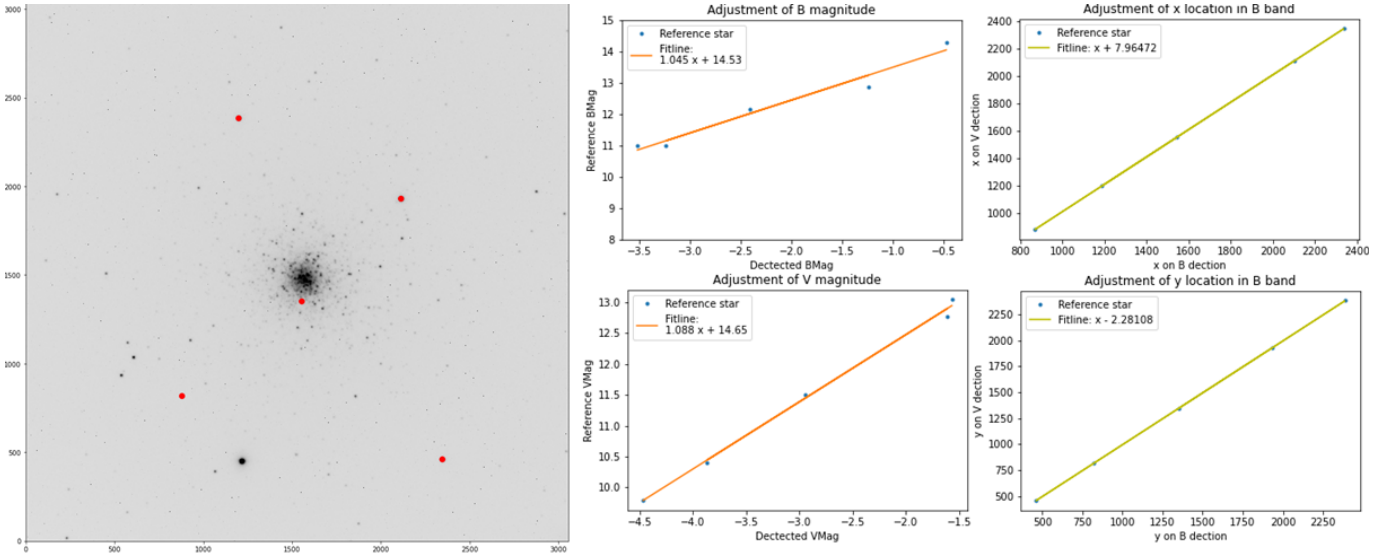

[1]Reference stars are in red dots. Apparently, only the center reference stars are inside M3. Other four corner reference stars are foreground stars. Since the calibration is on the apparent magnitude, distance does not effect calibration result.

Table 2: Reference Star Data on B,V Bands Observations and Match-Up in VIZIER

StarTag	RA	DEC	Bmag	Vmag	xcentroid	ycentroid	V_flux	B_flux	Bmag'	Vmag'
RightTop [1]	13:41:45.9732	28:27:16.700	11	9.8	2110.64	1929.39	61.18	25.59	-3.520	-4.466
LeftBottom[2]	13:42:43.7230	28:15:53.329	12.857	12.772	877.86	817.27	4.43	3.14	-1.243	-1.616
RightBottom[3]	13:41:35.465	28:12:11.848	12.147	11.501	2345.51	459.38	15.13	9.22	-2.412	-2.949
LeftTop[1]	13:42:28.5595	28:31:58.361	11	10.4	1197.21	2383.83	35.16	19.74	-3.238	-3.865
Center[4]	13:42:12.1238	28:21:21.825	14.285	13.038	1553.29	1349.01	4.25	1.55	-0.475	-1.570

VIZIER database souces: **[1]** ycho Input Catalogue, Revised version (Egret+ 1992) (Egret et al. 1992); **[2]** All-sky Compiled Catalogue of 2.5 million stars (Kharchenko+ 2009) 2001KFNT...17..409K (Kharchenko 2001); **[3]** The Tycho-2 Catalogue (Hog+ 2000) (Høg et al. 2000); **[4]** All-sky catalog of solar-type dwarfs (Nascimbeni+, 2016) (Nascimbeni et al. 2016).
Vmag, Bmag means the magnitude in VIZIER databases. Vmag', Bmag' refers the calculate raw magnitude by DAOPhot.

for the bias, our group subtract the master bias frame from the science and calibration frames. The master bias frame is created by combining multiple bias frames to reduce noise, and having a average value: 980.8946.

For flat correction, our group take 8 flat frames for each brands. In order to handle this variation and get a linear observation, a master flat frame was generated by combining the information from multiple flat frames, effectively creating a comprehensive representation of the illumination pattern and detector response. We normalize the master flats by dividing its mean. Finally, divide the calibration frames by the master flat frame to correct for pixel-to-pixel sensitivity variations. This process normalizes the response of the detector, effectively removing the effects of dust, vignetting, and other artifacts.

3.2. *Calibrations on Data*

After the data reduction process, several calibrations were performed on the B-band and V-band magnitudes, as well as coordinate calibration across the observations. The initial calibration involved adjusting the detected apparent magnitudes. In our study, we utilized the DAOPHOTFINDER algorithm (Stetson 1987) to calculate the magnitudes. We running DAOPhot on paramters: fwhm=3.0, threshold=3 standard deviation on the whole region of B,V bands observations. DAOPHOT searches images for local density maxima that have a peak amplitude greater than threshold and have a size and shape similar to the defined 2D Gaussian kernel. The Gaussian kernel is defined by the fwhm and other default parameters. The DDAOPHOT detects point sources and define its boundary. The algorithm sum up all the flux inside the region and establishes a relationship between flux and magnitude as following. It allowing us to determine the apparent magnitude for

the different stars observed.

$$magnitude = -2.5 \cdot log_{10}(flux)$$

Apparently, this relationship used by DAOPHOT does not involve the exposure time. As a result, this equation is limited to producing relative apparent magnitudes among different stars rather than providing absolute apparent magnitudes. In order to obtain calibrated apparent magnitudes, a constant shift is required to adjust the magnitudes derived from DAOPHOT.

In our study, we employed a method to adjust the magnitude values by utilizing "reference stars" that have recorded V-band and B-band magnitudes available in the VIZIER database. To ensure a robust calibration, we selected 5 prominent and evenly distributed stars from the observed images as our reference stars. These stars included the four corner stars and one central star, as illustrated in the graph (see Figure.1[1]). The graph visually represented the location adjustment across the B-band and V-band filters. To get the reference magnitude, We accessed existing data of B,V magnitude cross 4 data surveys (see Table.2). These reference stars provided a baseline for calibration purposes. To obtain the magnitude values in detection, we used the DAOPHOTFINDER algorithm to detect and measure the stars separately in the B and V bands.

By analyzing the relationship between the reference magnitudes and the algorithm's output, we derived a calibration relationship by performing linear fits on the B and V filter measurements to establish the regression lines(see Figure.1[2]). These regression lines represented the best-fit relationships between the calibrated B-band and V-band magnitudes.

$$B = 1.0454 \cdot B_i + 14.5349$$
$$V = 1.0880 \cdot V_i + 14.6505$$

With this derived regression lines, we were able to adjust the calculated magnitudes obtained from the DAOPHOTFINDER algorithm across both filters. This calibration relationship was then applied to all the calculated magnitudes obtained from the DAOPHOTFINDER algorithm.

The next produce is the calibration on x,y. Since we take two images separately and each time telescope will redirecting to the target coordinates, there would be a tiny instrumental offset when telescope pointing to the target. This leads to a tiny shift of images obtain by different time. Secondly, the calibration on the x,y location cross V, B band is also works in same way, obtain the DAOPHOTFINDERdetected x,y locations of references stars on both band, and then do linear regression fit on the on direction coordinate cross band. (see Figure.1[3]) We generate following relationship:

$$V_x = B_x + 7.9647$$
$$V_y = B_y + 2.2811$$

At this stage, all the necessary calibration steps completed, we have successfully prepared the data for further analysis. The calibrated magnitudes, positions, and other relevant information of the detected stars are now available. This enables us to working some statistic result on the observations and also generating a color-magnitude diagram (CMD) based on the observations.

3.3. *Color index match-up of M3*

This part is not directly related to calibration, but it considered as a preparing work for the generate stellar isochrone in the later on CMD. Since the next part would be result and analysis, it better to place this part under the reduction and calibration section.

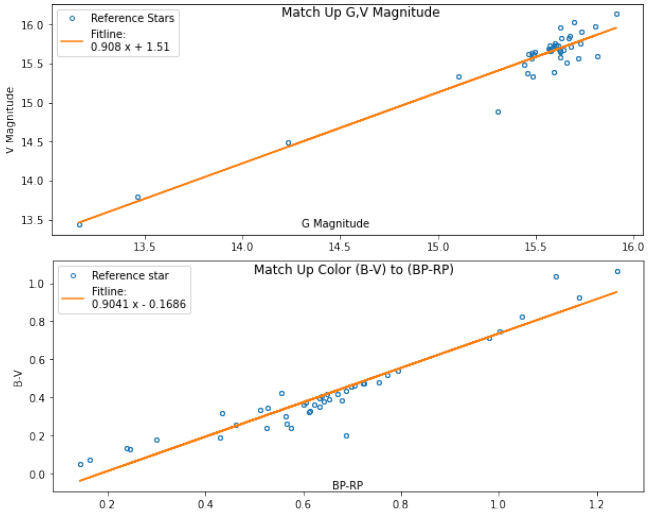

Figure 2: Cross band match up on BP,RP,G,V,B

$$V = 0.908 \cdot G + 1.51$$
$$(B - V) = 0.904 \cdot (BP - RP) - 0.1686$$

We obtains the stars (with BP,RP,G magnitude) in data survey "Mapping hot luminous stars in the Galaxy (Zari+, 2021)"(Zari et al. 2021), and cross match up the stars (V,B magnitude) in data survey " Gaia EDR3 and Johnson-Kron-Cousins standards (Pancino+, 2022)"(Pancino et al. 2022) with a tolerance 2 arcsec. We ggot 88 stars match-up, which gives a relative rubust result about the relationship between (BP-RP) and

Figure 3: The Detected Stars Location Mapping [1] The CMD of M3 with Color(B-V) On ARCSAT observation [2]

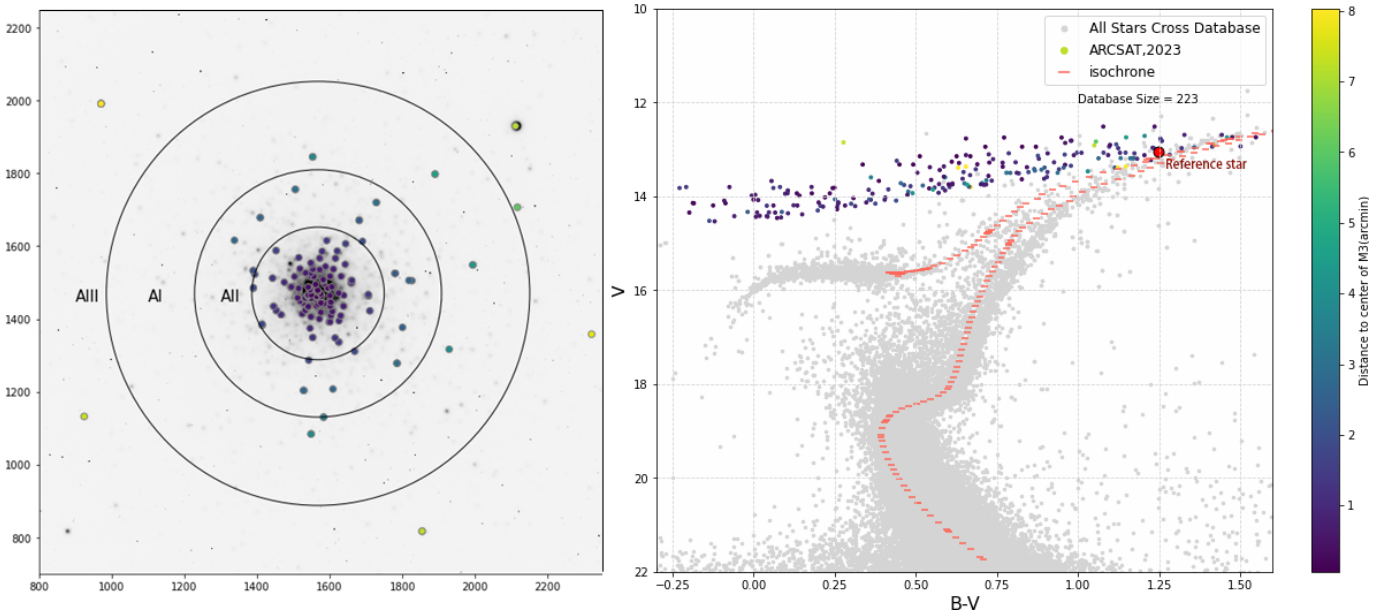

[1]Map of the survey regions in M3. The area AI, with radial distance $3.5' < r < 6.0'$ consider as outer region of M3. The area AII, inner annulus, with $2.0' < r < 3.5'$. The area AIII external square with $6 < r < 8.1'$. Consider, AI and AII is the mainly studied region of M3. Color indicates the distance to center of M3, and is correlated to the CMD map.
[2] Purple dots are data taken from ARCSAT(they has clear low boundary which will be discussed).Red dot is the referece star. Gray dots are referecne data from 6 VIZIER data surveys include M3 (Stetson et al. 2019) (Pancino et al. 2022) (Hartman et al. 2005) (Henden et al. 2016) (Cacciari et al. 2005) (Benkő et al. 2006). Stellar isochrone shows by pink line, which generated based on following constant of M3: [Fe/h] = -1.57, distance = 11.57kpc, age = 11.57Gyr.

(B-V), and Gmag and Vmag. The linear regression relationship fitted is above, and it will used to convert the generate (BP-RP) vs G stellar isochrone to (B-V) vs V isochrone. The stellar isochrone will be shown up as a pink line on graph.

4. PHOTOMETRIC RESULT AND ANALYSIS

4.1. *Photometric Result*

The independent detection on two bands by DAOPHOTFINDER is : on B bands, there are 1240 stars be detected, with an average magnitude 13.8748 ± 0.7182. On V bands, there are 1494 stars be detected, with an average magnitude 13.9167 ± 0.7197. Both of them are significantly higher than the average reference apparent magnitude of M3. Foreground stars would be one influencing factors. To eliminate its impact, the following result has limitation on location.

We match up the stars on B,V bands with an tolerance radius in 2 pixels($1.237''$). It cross matches up 258 stars as total. Only small portion (17.2%) of detected stars be match up. This relatively low percentage of matched stars can be attributed to the fact that many stars are only noticeable or detectable in one of the observed bands depending on their intrinsic color.By clarify, the basic shape of CMD already determined by calibration process, increase the match up tolerances to 2 arcsec could improve the match-up percentage, but wouldn't improve final CMD result. It only makes a denser CMD based on current shape. On the other hand, the current detection at the inner region of M3 is dense and blur(see Figure.3[1]), in order to maintain the relative reliable detection, it's better to keep the tolerance range as 2 pixels. S For those matched stars, 223 stars are in the region of M3 which is $r < 8.1'$ (Brosche et al. 1999)(see Figure 3). According to the region classification by (Buonanno et al. 1994), among those stars located inside M3, 26 stars are in inner annulus AII region ($2.0' < r < 3.5'$), 9 stars are in AI region, and 45 stars are in external square AIII region ($6 < r < 8.1'$).

Apparently, most stars (178 stars, 79%) are in the region $r < 2.0'$, which was consider as the over-dense region that was not studied by original papers (Paez et al. 1990) (Buonanno et al. 1994) due to the limitation on resolution. Current papers (Massari et al. 2016) (Kumar et al. 2023) (Hamrick et al. 2021) are not providing the specific distance infomation on their result, probably because the resolution has been

improved a lot. However, nowadays, the region $r < 1.1'$ is still be considered as a dense core of M3. This leads a hidden risk on our final result. In order to eliminate the effect, our graph providing figure of locations and a color-map on the distance to M3's center along the CMD. Please consider the green-blue parts as the more reliable region.

Finally, we generated the Color magnitude diagram (see Figure 3[2]) based on observation on 22th Apirl in ARCSAT. All stars on CMD are selected in $r < 8.1'$ which is inside the region of M3, .

the average V magnitude is about 13.577 ± 0.5740 which is beyond all other survey reported. The reddening $E(B-V) = 0.5886 \pm 0.4684$, which is beyond 0.01 reported (Harris 2010) and 0.0 reported by (Valcarce & Catelan 2008), and 0.015 reported by (Preet Kaur & Joshi 2022). But least its uncertainty include those reported values.

4.2. *Analysis*

Obviously, the produced result (no matter statistic quantities nor graphs) does not agree with previous surveys. We got a dramatic error on result. Thus, it' hard to establish any astronomic Analysis based on the result and the sections below will discuss about why our result looks wrong.

The following discussion covers: the telescope and exposure time used, the choose on source detecting photometry,the input parameter used in DAOPhot, the tolerance range on coordinate match-up cross bands, and the decision making on reference star. For all five of these factors, We will talk about why we have current decision and whether making a change could improve the result or not.

For the equipment we used, our telescope is 0.5m radius, and exposure time is 600 second. Firstly, radius with 0.5m is not a huge radius, but it definitely enough for our study on M3. Hamric's group (Hamrick et al. 2021) usd 0.4m telescopes of Las Cumbres Observatory Global Telescope,and got a great result on M3. On the other hand, exposure time with 600 seconds is also a reasonable time. Even though most of pixels located inside the M3 are under-exposed (about 3000/65000), cross compared with other surveys (mostly using 120s or 300s exposure time and got beautiful result), it is a reasonable time. Also, the impact by weather is also limited. The errors occurs on relative flux cross stars. It is rare if existing a tiny piece of cloud covers certain area of observation and leaves other area clear. Therefore, for this part, we believe no factors on observations impacts the final result.

The second is the detecting photometry we used. We currently use DAOPHOT, but there are three candidates of detecting algorithm we could used which are providing by python package PHOTUTILS . The first one is PSF Photometry(Anderson & King 2000)(Bryson et al. 2010). The PSF photometry itself means taking Point Spread Function (PSF) to be the infinite resolution and infinite signal-to-noise flux distribution from a point source on the detector, after passing through optics, dust, atmosphere, etc. Thus, it is a simulation tool(maybe). Combined it with DAOPHOT, it produce a *DAOPhotPSFPhotometry* function. This is a common used detecting photometry, most of the recent works (Kumar et al. 2023)(Hamrick et al. 2021) on M3 are base on it. However, it requires World coordinates system(WCS) for fit data. Since our B bands fit loose WCS information and STRONOMETRY not works on that, our group only have one proper WCS fit. Thus, we cannot using PSF. The second is Aperture Photometry(199 1992), Aperture photometry is a widely used technique in astronomy for measuring the flux or brightness of astronomical sources, particularly point-like sources such as stars. It involves measuring the amount of light captured within a specific aperture or circular region around the source of interest. Unfortunatly, Aperture photometry also requires WCS, which couldn't be used by our observation. The third one is DAO finder algorithm which has been introduce in detail in section of calibration. Beside those packaged photometry in DAOPHOT, there are a number of recent developed decting algorithm, like using deep learning on source detection (Vafaei Sadr et al. 2019). These algorithms discussion about algorithm performance and mathematics prove in paper, but doesn't providing a user-friendly package to use. It's impossible to implement them on our data. As a conclusion, theDAOPHOT is the only detecting algorithm we could use. It is a classical and legend algorithm,but it is also a bit obsolete. There are some advanced version of Dao finder based on new functions, but they cannot be applied since we lack WCS on B bands. If we have a chance to use other functions, it probably has a noticeable improve on result. Especially fix the problem majority of detection crowed at "relative magnitude" = 0 (show up on the CMD is the bottom of dots shows a solid boundary). It seems the algorithm has low resolution on calculating flux, and generate most flux approaching zero.

The third part is about the parameter we used on DAOPHOT. The parameters are: fwhm=3.0, threshold=3 standard deviation. The value of fwhm is a suggested value, there nothing interesting about

it. The parameter 'threshold' indicates if any group of pixels with size of fwhm exceed this threshold, the algorithm will detects it as a point sources, and search around it to build up a profile of this star. It seems if we lower the threshold, we will getting more dim star and that providing more dots on lower region on CMD. The logical mistake here is that the lowest flux DAOPHOT can detect is zero, and for currently graph, there are already a huge portion of stars crowed at flux = 0 region, which forms a distinguishable and clear boundary at the bottom(see Figure.3[2]). Decreasing the threshold only makes more stars crowed at bottim boundary, and lead the graph more ugly. On the other hand, increase the threshold wouldn't improve the distribution on CMD yet. This conclusion is made by testing different values on threshold. Increasing threshold can deceases total detected size, and make the dots distributed a bit separated or dispersed, but did limited effect on the shape of CMD(It still a approximate linear line). The 3 standard deviation be picked since it makes CMD moderately distributed compare to other values. This is the best we can do on it. Thus, we conclude changing the parameter on DAOPHOT won't improve the output CMD.

The fourth factor is the tolerance value of coordinate match-up cross B,V bands. This value has been brief discussed in calibration section. Increase the tolerance lets more stars be matched, but would not change the shape of distribution of CMD. It only makes total distribution denser. On the other hand, it's risky to rise the tolerance, since this greatly bonus the number of matched stars in dense core of M3. At the center of M3, it contains many blurred crowed stars, so this increases the percentage of miss matched stars, which will further polluted our result. On the other hand, decreases the tolerance to 1 pixel wouldn't improved CMD yet, and it only matched 30+ stars, which is not a reasonable size of sample to study.

The last factor is the decision making on choosing reference stars. By tracking the location of reference star on CMD (see Figure 3[2]), our group found this might be one of primary element influencing the final result. As discussed in calibration section, 5 reference stars are chosen based on their locations: 4 corner stars, and 1 central star. This decision is mainly aiming to calibrate on coordinates. Thus, you would find out 4 corner stars are foreground stars. Since they are used for calibrating on apparent magnitude, and whether they are inside M3 or not doesn't effect the result. In addition, since they have evenly distributed "relative apparent magnitude" (see Figure1[2]). Our group thought this is a great combination of reference stars. However, according to the CMD, there are two main problems, the first one is lacking reference stars inside M3. As the CMD show, the only portion our data overlap with other surveys is right part which is stuck by the reference star. The reference star does a notable job on calibration. On the other hand, the left side which is not hold by a reference star, fly away from the reference. Thus, to include more reference stars that would occur on the resulted CMD is necessary. The next issue is lacking of blue reference stars. Our original works only consider the calibration on V,B bands correlation separately. The data on both raw Vmag and raw Bmag is disperse distributed, but our group doesn't realize the B-V magnitudes for all reference stars are positive. Moreover, 3 stars has $B - V = 0.5$, and 2 stars has $B - V = 1.2$.(B-V)magnitude are group in 2 values, and hot stars are underrepresented. Thus adding more hot reference star inside the M3 is necessary, and it has a large chance to make a considerable effect on the final CMD.

As a conclusion, by analyzing these five factors,our group find out changing the detecting algorithm and adding more blue reference stars from M3 are the most practicable and efficient way to improve the result. Based on a correct detecting and calibration, increase the tolerance of match-up and increase the threshold would generate more precise result, but also cut down the sample size of study.

Finally, short discuss about what would be the possible result after did improvement: our result probably detects the red giant branch, asymptotic giant branch and horizontal branch. What it specifically included depending on location of adjusted data. We hope our result will looks similar to one of the following surveys (see Figure.4). One of our group hypothesis is that final result would looks like the CMD at the top row of Figure.4, but that requires a extreme small regression slope on calibration on B,V band. Another more possible guess is it will looks like Herden's CMD which is middle CMD at second row.

Figure 4: The Color Magnitude Diagrams of M3 with Color(B-V) Across Multiple Data Surveys on VIZIER

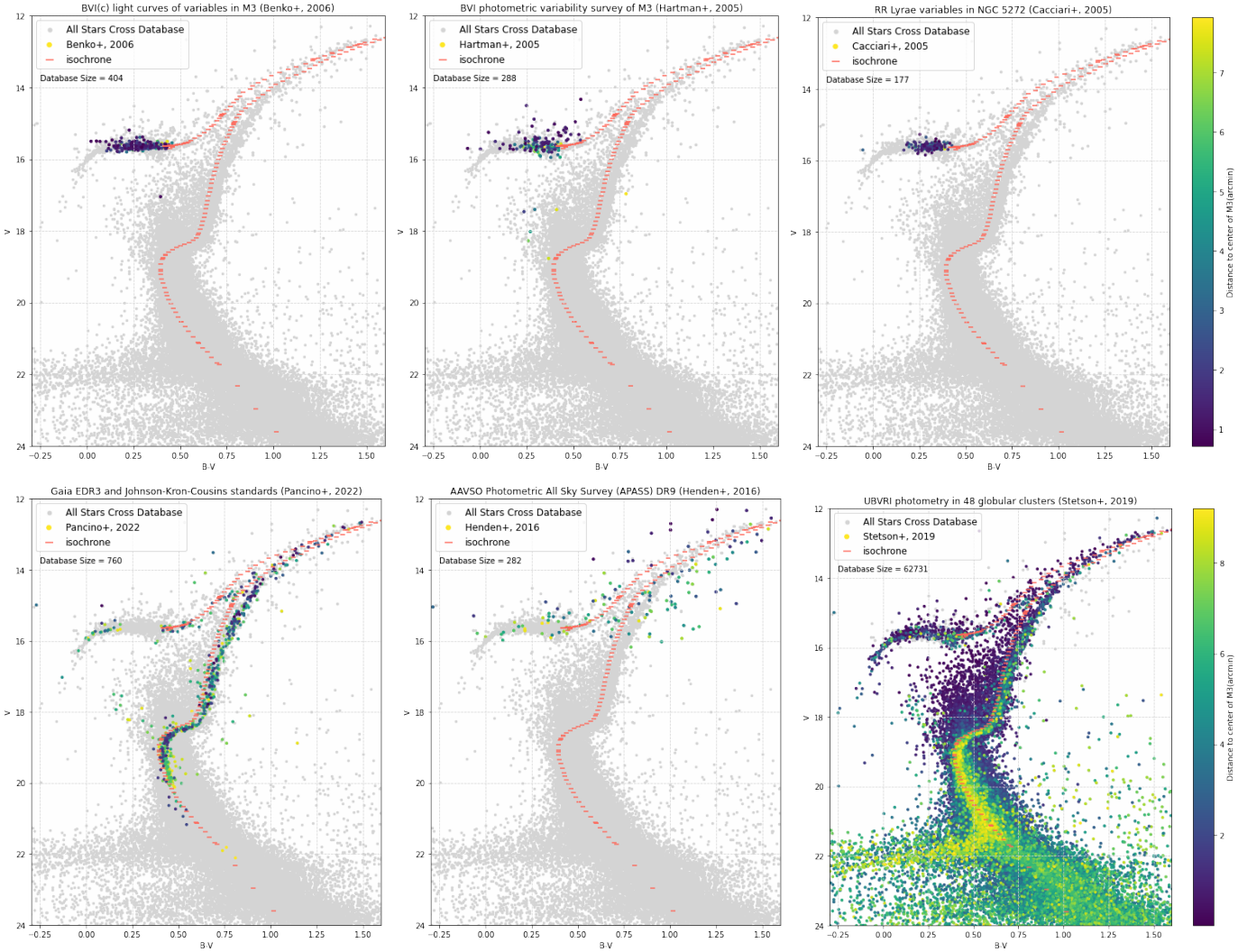

The VIZIER database sources: [1,1](Benkő et al. 2006) BVI(c) light curves of variables in M3 (Benko+, 2006) [1,2](Cacciari et al. 2005) RR Lyrae variables in NGC 5272 (Cacciari+, 2005) [2,1](Hartman et al. 2005) BVI photometric variability survey of M3 (Hartman+, 2005) [2.2](Henden et al. 2016) AAVSO Photometric All Sky Survey (APASS) DR9 (Henden+, 2016) [3,1](Pancino et al. 2022) Gaia EDR3 and Johnson-Kron-Cousins standards (Pancino+, 2022) [3,2](Stetson et al. 2019) UBVRI photometry in 48 globular clusters (Stetson+, 2019) All Stars inside 8.1 arcmin radius region of M3 center from above survey has been selected and shown. Isochrone are fit based on following constant of M3: [Fe/h] = -1.57, distance = 11.57kpc, age = 11.57Gyr.

5. CONCLUSION

In this study, we conducted a photometric analysis of the globular cluster M3, utilizing observations in the B and V bands and generating a Color-Magnitude Diagram (CMD) based on the B-V color index. By employing the DAOPhot algorithm for star detection and performing a cross-match between the two bands, we obtained photometric measurements and identified individual stars within the cluster.

By comparing our CMD with previous studies, we acknowledge a few discrepancies that may arise from variations in observational data, photometric calibration, or stellar evolution models. These inconsistencies highlight areas for improvement and suggest the need for further investigations to enhance our understanding of M3's properties and dynamics. Since our group doesn't makes any reasonable result, it is impossible to generate a astronomic theory based on it, these paper is mainly a half processed report.

Future works our group could do is apply improvement we provide on section of analysis. like switch the detecting algorithm to FPSDAOPhot and adding more high luminosity reference stars, decreasing the tolerance and increasing the threshold. If a reasonable data is achieved, we could make a analyse on stellar isochrone and also those constant generated by isochrone like Age, distance, [Fe/h], [M/H],matellicity Z, etc.

There are serverl other topic to do on M3:Further refining the photometric analysis of the M3 CMD can provide more accurate and precise measurements of stellar magnitudes and colors. This can involve improving the data reduction techniques, optimizing the calibration process, and incorporating advanced algorithms for star detection and photometry. Achieving higher signal-to-noise ratios and reducing systematic uncertainties will enhance the reliability of the CMD and enable more detailed investigations.Incorporation of Additional Observational Bands: Expanding the observations to include additional bands, such as infrared or near-ultraviolet wavelengths, would provide a more comprehensive view of the stellar populations in M3. These additional bands can reveal unique features related to stellar properties such as temperature, metallicity, and chemical composition. Incorporating these bands into the CMD analysis would enrich our understanding of M3's stellar populations.

In conclusion, our study successfully generated a CMD for the globular cluster M3 based on B and V band observations and the B-V color index. The disagreement between our results and previous studies indicates we better adjust our result. By identifying discrepancies and discussing potential improvements, we lay the foundation for future investigations that will advance our understanding of M3 and other globular clusters in the universe.

REFERENCES

1992, Astronomical Society of the Pacific Conference Series, Vol. 23, Astronomical CCD observing and reduction techniques

Anderson, J., & King, I. R. 2000, PASP, 112, 1360, doi: 10.1086/316632

Benkő, J. M., Bakos, G. Á., & Nuspl, J. 2006, MNRAS, 372, 1657, doi: 10.1111/j.1365-2966.2006.10953.x

Brosche, P., Odenkirchen, M., & Geffert, M. 1999, NewA, 4, 133, doi: 10.1016/S1384-1076(99)00014-7

Bryson, S. T., Tenenbaum, P., Jenkins, J. M., et al. 2010, ApJL, 713, L97, doi: 10.1088/2041-8205/713/2/L97

Buonanno, R., Corsi, C. E., Buzzoni, A., et al. 1994, A&A, 290, 69

Cacciari, C., Corwin, T. M., & Carney, B. W. 2005, AJ, 129, 267, doi: 10.1086/426325

Egret, D., Didelon, P., McLean, B. J., Russell, J. L., & Turon, C. 1992, A&A, 258, 217

Goldsbury, R., Richer, H. B., Anderson, J., et al. 2010, AJ, 140, 1830, doi: 10.1088/0004-6256/140/6/1830

Hamrick, P., Bansal, A., & Tock, K. 2021, JAAVSO, 49, 192

Harris, W. E. 2010, arXiv e-prints, arXiv:1012.3224, doi: 10.48550/arXiv.1012.3224

Hartman, J. D., Kaluzny, J., Szentgyorgyi, A., & Stanek, K. Z. 2005, AJ, 129, 1596, doi: 10.1086/427252

Henden, A. A., Templeton, M., Terrell, D., et al. 2016, VizieR Online Data Catalog, II/336

Høg, E., Fabricius, C., Makarov, V. V., et al. 2000, A&A, 355, L27

Kharchenko, N. V. 2001, Kinematika i Fizika Nebesnykh Tel, 17, 409

Kumar, R., Pradhan, A. C., Sahu, S., et al. 2023, MNRAS, 522, 847, doi: 10.1093/mnras/stad1009

Massari, D., Lapenna, E., Bragaglia, A., et al. 2016, MNRAS, 458, 4162, doi: 10.1093/mnras/stw583

Nascimbeni, V., Piotto, G., Ortolani, S., et al. 2016, MNRAS, 463, 4210, doi: 10.1093/mnras/stw2313

Paez, E., Straniero, O., & Martinez-Roger, C. 1990, A&AS, 84, 481

Pancino, E., Marrese, P. M., Marinoni, S., et al. 2022, A&A, 664, A109, doi: 10.1051/0004-6361/202243939

Preet Kaur, K., & Joshi, P. S. 2022, arXiv e-prints, arXiv:2209.03019, doi: 10.48550/arXiv.2209.03019

Stetson, P. B. 1987, PASP, 99, 191, doi: 10.1086/131977

Stetson, P. B., Pancino, E., Zocchi, A., Sanna, N., & Monelli, M. 2019, MNRAS, 485, 3042, doi: 10.1093/mnras/stz585

Vafaei Sadr, A., Vos, E. E., Bassett, B. A., et al. 2019, MNRAS, 484, 2793, doi: 10.1093/mnras/stz131

Valcarce, A. A. R., & Catelan, M. 2008, A&A, 487, 185, doi: 10.1051/0004-6361:20078231

Zari, E., Rix, H. W., Frankel, N., et al. 2021, A&A, 650, A112, doi: 10.1051/0004-6361/202039726